JOURNAL OF MECHANICAL ENGINEERING AND SCIENCES
ISSN: 2289-4659 e-ISSN: 2231-8380
VOLUME 19, ISSUE 2, 2025, 10642 - 10652
DOI: https://doi.org/10.15282/jmes.19.2.2025.6.0834

RESEARCH ARTICLE

Finite element analysis of hip implant using additive manufacturing materials in different loading conditions

A. A. Noman[1], M. S. Shaari[1]*, M. R. M. Akramin[1], K. S. Tan[2]

[1] Faculty of Mechanical and Automotive Engineering Technology, Universiti Malaysia Pahang Al-Sultan Abdullah 26600, Pekan, Pahang, Malaysia
Phone: +6094315366

[2] Oryx Advanced Materials Sdn Bhd, Plot 69(d) & (e), Lintang Bayan Lepas 6, Bayan Lepas Industrial Zone, Phase 4, Bayan Lepas, 11900 Penang, Malaysia

ABSTRACT - A hip implant is a crucial medical device designed to restore mobility and relieve pain for an individual with a hip joint with degenerative diseases or injury. Conventional manufacturing techniques have limitations in producing personalized implants. In contrast, additive manufacturing (AM) offers a solution by enabling the production of hip implants using biocompatible materials, such as Ti-alloy, CoCr-alloy, and Mg-alloy. Ti alloys are used for their superior biocompatibility and mechanical performance. This study aims to utilize a computer-aided design file in finite element analysis (FEA) to predict implant stress distribution, deformation, and potential biomechanical performance. The methodology includes designing the hip implant with CAD software and using Ansys to assess the mechanical performance of hip implants using Ti-6Al-4V, an AM material, at four different loading conditions. The results indicate that the total deformation at four different loadings is as follows: sitting, 0.15%; standing, 0.17 mm; walking, 0.21%; and jogging, 0.33%. The equivalent von Mises stresses of the hip implant while sitting: 288.83 MPa, standing: 339.8 MPa, walking: 423.73 MPa, and jogging: 650.93 MPa. Additional analysis of shear stresses for the hip implant while sitting: 59.738 MPa, standing: 70.28 MPa, walking: 84.556 MPa, and jogging: 134.630 MPa. Based on the result, maximum deformation, equivalent stress, and shear stress are predicted to be highest while jogging compared to other activities due to the highest load acting on the hip implant, and equivalent stresses are less than the material's yield strength and similarly shear stresses are less than the material's shear strength that indicates the design is safe under physiological loadings. In conclusion, this study successfully implemented the FEA of hip implants using AM materials to achieve potential mechanical performance. The integration of AM and FEA holds promise for the future of modern hip replacement surgery.

ARTICLE HISTORY
Received : 25th Nov. 2024
Revised : 27th May 2025
Accepted : 03rd June 2025
Published : 30th June 2025

KEYWORDS
Finite element analysis
Hip implant
Additive manufacturing
Biocompatibility
Total hip replacement

1. INTRODUCTION

Hip implant surgeries have given quality of life to millions of patients who have had several hip illnesses, such as osteoarthritis, rheumatoid arthritis, and traumatic fractures [1]. The design and performance of hip implants are developed to preserve hip stability, reduce discomfort, and restore patient mobility [2]. Generally, a hip implant contains a total of three parts: an acetabular cup, a femoral head, and a femoral stem. The femoral stem part is fully inserted into the femoral bone. On the other hand, the femoral head and acetabular cup adjust with the hip joint to mimic the ball-and-socket joint activity. Figure 1 illustrates the various components of the hip implant. Traditional hip implants have been predominantly produced using conventional machining techniques for a long time, including CNC machining, casting, and forging. Although these methods can manufacture hip implants, the process involves material wastage, extensive post-processing, and limited design flexibility. Therefore, developments in additive manufacturing (AM) have been increasing the potential of day-to-day production in different manufacturing industries. AM uses a layer-by-layer method to manufacture the final product [3,4]. Compared to conventional manufacturing techniques, AM has many benefits, such as improved manufacturing flexibility, less material waste, and higher design freedom. Industries such as automobiles, aerospace, and healthcare have been benefiting from this newly introduced method of manufacturing products [5]. As a result, AM becomes the potential manufacturing process for medical implants, especially hip implants. By creating patient-specific designs and incorporating bioabsorbable implant additives, manufacturing has the potential to completely transform the orthopedic implant industry and revolutionize the production of hip implants. AM processes, such as selective laser melting (SLM), selective laser sintering (SLS), stereolithography (SLA), electron beam melting (EBM), and direct metal laser sintering (DLMS), are widely used in metal additive manufacturing processes [6]. Figure 2 shows the manufacturing process of hip implants through AM. It demonstrated the schematic diagram of the printing process of the hip implant using laser power. When a patient requires an implant, the process begins with medical imaging data. For example, computer tomography (CT) scans and magnetic resonance imaging (MRI) can be used to design the implant through computer-aided design (CAD) software [7, 8]. After obtaining the CAD data, it will be converted into an STL file and then uploaded into the printing machine's computer to print the model. The machine utilizes CAD data to fabricate the

*CORRESPONDING AUTHOR | M. S. Shaari | ✉ shamil@umpsa.edu.my

model, using a laser beam to melt the powder metal in the powder bed and create a solid layer. After finishing one layer, the machine spread the powder metal, and then the laser melted it to join the layers together. This process continues until the printing process finishes. At this stage, the most important factor is selecting suitable materials for hip implants based on their biocompatibility.

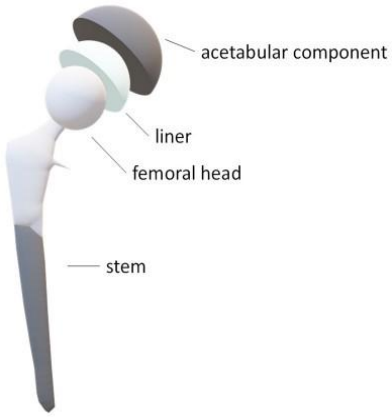

Figure 1. Different parts of the hip implant [9]

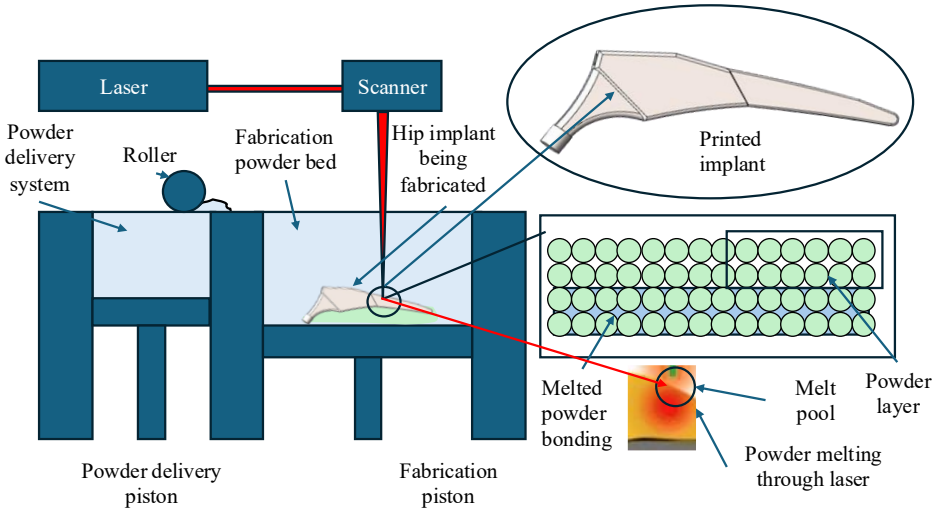

Figure 2. Hip implant manufacturing through AM

Materials like CoCr-alloy, Ti-alloy, Mg-alloy, composite materials, and ceramics are the most commonly used biocompatible materials for hip implants [10]. Sometimes those materials also face difficulties like stress shielding and wear debris [11, 12-15]. Therefore, the most convenient approach to the manufacturing of hip implants can be achieved by the integration of AM and finite element analysis (FEA). It helps to achieve the optimal design to prevent problems such as stress shielding and improve the biomechanical strength of the hip implant [16,17]. Hence, when it comes to designing the implant to reduce stress shielding and achieve higher biomechanical strength, FEA plays a vital role [2,18]. FEA is an advanced computational method that provides the freedom to assess the mechanical performance of the implant, identify design defects, failure mechanisms, and optimize design possibilities, as well as post-process for a perfect stress-strain distribution to minimize stress shielding effects [19]. Ansys, Abaqus, and Nastran are commonly used FEA software for this type of computational analysis [20, 21]. In summary, the integration of hip implant design, AM, and FEA presents a strong advancement in modern orthopedic implant technology to provide quality of life for patients. However, there are limited comprehensive studies that have been conducted regarding the FEA of hip implants using AM materials under different loading conditions. So, this study aims to perform FEA on hip implants made of additive manufacturing materials to evaluate the performance of AM hip implants by examining their mechanical behavior under different loading conditions.

2. MATERIALS AND METHODS

The research methodology starts with CAD modeling and ends with FEA results. It consists of five steps, beginning with a CAD drawing generated using SolidWorks. After that, AM material is selected based on its biocompatibility and mechanical properties. Then, an FEA of the hip implants will be created using Ansys. Subsequently, static structural analysis is performed to investigate the deformation, stress distribution, and mechanical behavior of the hip implant. These five steps will be explained in the following subsection.

2.1 CAD Drawing

The hip implant design is created using SolidWorks, which was selected due to its capability to design more accurate geometry and models. The designed file was then saved in a specific supported format for further analysis using FEA software [22]. After the CAD model was taken and imported into Ansys. During the import process, it is ensured that the correct geometry is imported to facilitate further processing and analysis. In this study, the length of the implant CAD model is 161.30 mm, the thickness of the implant is 8mm, the diameter of the implant head is 11.5 mm, and the length of the stem is 121.83 mm. Details of the dimensions are represented in Figure 3. The dimensions were taken by following the reference of the adult patients' femoral bone dimensions and following the ISO 7206-4 hip implant specimen testing standard.

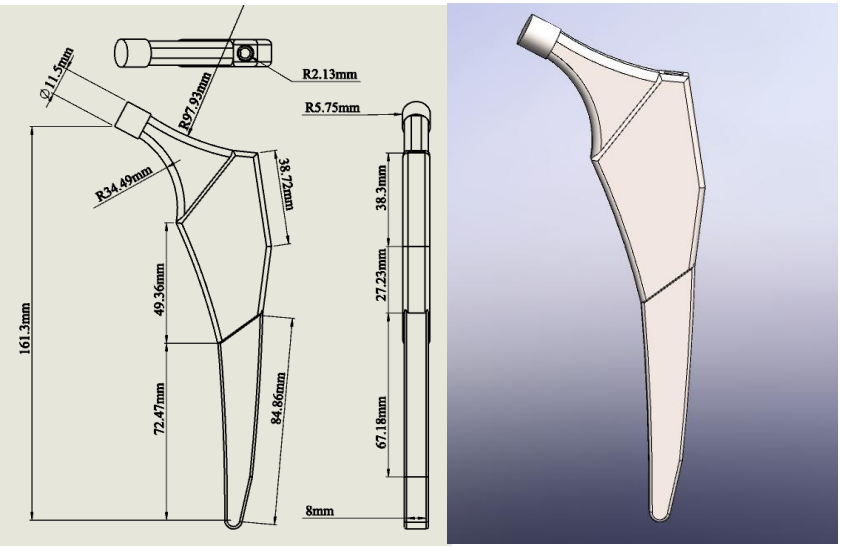

Figure 3. Design and dimensions of hip implant

2.2 Selection of the Materials

The process of selecting the right material for hip implants is crucial, as it significantly impacts the implant's lifetime and performance [23]. To ensure that the implant functions properly within the body, the materials selected must meet stringent specifications for biocompatibility, mechanical strength, wear resistance, and corrosion resistance [24]. The correct materials can provide the mechanical stability required to sustain everyday activities, improve the implant's integration with the bone, and reduce wear particles that might cause issues [25]. The performance and longevity of hip implants are continuously improved by advances in materials science, which enhances the quality of life for those who require hip replacement surgery. Nowadays, titanium alloy (Ti), cobalt chromium(CoCr) alloy, magnesium-based alloy, and ceramics are used as implant materials [26]. CoCr and Ti alloys are widely used biomaterials for hip implants due to their higher biocompatibility, wear, and corrosion resistance. According to the literature, Ti-6Al-4V is suitable due to its higher mechanical performance and biocompatibility compared to other materials [27]. In this paper, Ti alloy (Ti-6Al-4V) is used to analyze the hip implant design. Table 1 shows the material properties of Ti-6Al-4V.

Table 1. Material properties of Ti-6Al-4V

Young Modulus (GPa)	Poisson Ratio	Tensile Yield Strength (MPa)	Ultimate Tensile Strength (MPa)	Density (kg/m^3)
113.8	0.342	880	950	4430

2.3 Finite Element Analysis

FEA is a computer method that breaks down a complex model into smaller, manageable finite elements of design to identify responses to external stresses, heat, and other physical phenomena. The method involves specifying the geometry, material properties, and boundary conditions, creating a mesh of finite elements, and solving the resulting equations to determine variables such as stress, displacement, and crack growth behavior [28-31]. FEA is widely utilized in various engineering domains, providing precise insights and reducing the need for physical prototypes, and it demands substantial skill and computational resources. Several tools of FEA are used to study the behavior of bones and joints under different loading conditions. Apart from them, Ansys is a highly recommended tool for FEA and simulation because it can simulate complex CAD models [22]. To verify the final element model, a comparison was conducted with the previous study by Shenoy et al. [32], which validated their findings that a hip implant experiences an equivalent von Mises stress of 207.207 MPa under 2300.5 N loads. This study also followed the same boundary conditions and materials properties and geometry to verify the results with the previous study, where it is found that the hip implant experiences 204.1 MPa equivalent von Mises stress, which is slightly less than the previous value it is because of the different versions of the software and computer processing capacity. The percentage error between the current study result is approximately 1.52%.

2.3.1 Meshing

The mesh is generated for the hip implant using FEA software (Ansys- manufacturer: Ansys Inc.; country: Canonsburg, Pennsylvania, US). However, the meshing process involves dividing the CAD model into several smaller parts, allowing for analysis through Ansys [33, 34]. During meshing, it is ensured that the mesh quality of the model is fine and that there are no unmeshed parts, as the quality of the mesh significantly affects the accuracy of the FEA simulation. In this study, the independent mesh is generated to get an accurate analysis result. The first mesh convergence analysis was conducted to determine the optimal mesh for subsequent analysis. The mesh quality was confirmed from mesh metric quality, element quality, and skewness. According to the meshing scale, the selected mesh quality falls within the fine mesh range because the material quality is greater than 85% based on skewness and aspect ratio criteria. The mesh convergence study confirms that further refinements did not significantly affect the results, which confirmed that the mesh resolution was sufficient for reliable stress and strain predictions. The transition ratio of 0.272 mm was used to control mesh growth between the fine and rough regions, ensuring smooth changes in material size. The final mesh size, evaluated based on mesh convergence, is 5 mm, which yields better results. The number of nodes is 11888, and the number of elements is 6685, respectively. Figure 4(a) illustrates the mesh convergence study for selecting the final mesh, and Figure 4(b) displays the generated mesh on the implant design, where the element size is programmatically controlled. The mesh size range was chosen to be from a minimum of 0.5 mm to a maximum of 7 mm. The minimum size was selected as 0.5 mm due to the computer's processing power limitations. Finally, the maximum size of the mesh was 7mm because, after this mesh size, the geometry contains more sharp edges and deformed shapes.

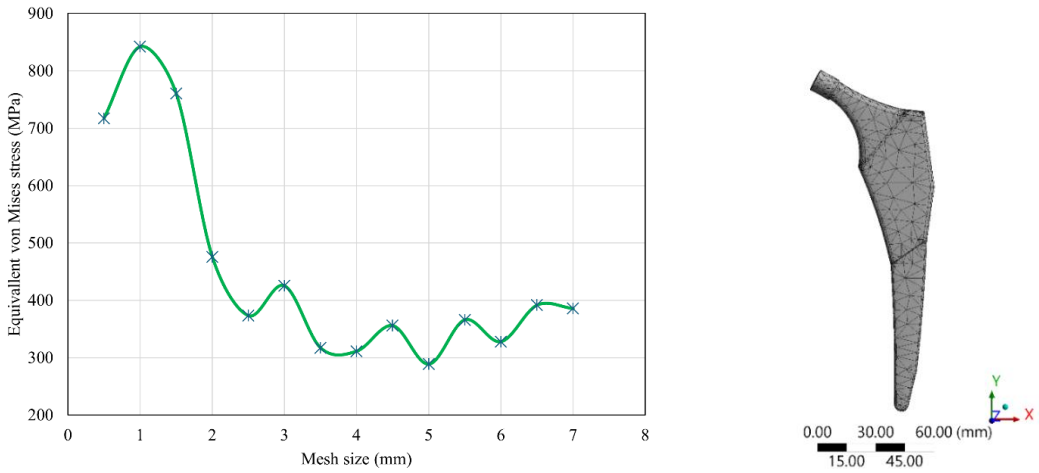

(a) (b)

Figure 4. (a) Mesh convergence study and (b) Meshing on the hip implant model

2.3.2 Boundary conditions

To simulate real-world interactions in the patient's body, boundary conditions were applied to the hip implant to study the physiological forces, specific loads, and supports. By correctly applying the boundary conditions, FEA enables the calculation of implant behavior in realistic settings, contributes to the best design, and ensures safety and efficiency in hip replacement surgery patients [35]. In this paper, the implant was subjected to four loading conditions (four different loads: sitting, standing, walking, and jogging) applied to the femoral head region in the negative y-direction, and a fixed support was applied to the bottom edge of the implant using the global coordinate system. These loads represent the forces experienced by the implant during normal physiological activity. By applying specific loading conditions, the aim was to understand the mechanical behavior of hip implants in practical situations. Those four physiological loads were derived from a published paper in which the researcher analyzed different types of physiological loads acting on the femoral head in a patient's daily life [36]. Table 2 shows the four different loads applied to the hip implant, where the sitting load is 1360 N, the standing load is 1600 N, the walking load is 1925 N, and the jogging load is 3065 N, respectively. Finally, Figure 5 represents the boundary conditions of the hip implant, where it shows the applied load and fixed support [21][36]. Where point A represents the fixed support and point B represents the applied force on the implant head.

Table 2. Applied loads on the hip implant [21, 35]

Types of Loads	Load (N)
Sitting load	1360
Standing load	1600
Walking load	1925
Jogging load	3065

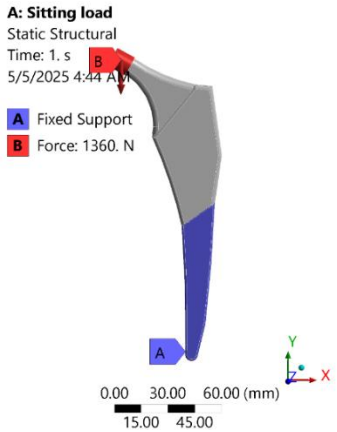

Figure 5. Boundary conditions of loading and fixed support

3. RESULTS AND DISCUSSION

3.1 Total Deformation

Figure 6 illustrates the total deformation of the hip implant under four different loading conditions: sitting load, standing load, walking load, and jogging load. The results for deformation when sitting are 0.235 mm, for standing are 0.276 mm, for walking are 0.335 mm, and for jogging are 0.530 mm. From the results, it is observed that the percentage of change is as follows: sitting, 0.15%; standing, 0.17 mm; walking, 0.21%; and jogging, 0.33%. Based on the results, the total deformation of hip implants is increasing with the increase in applied physiological loads. Hence, the more forces subjected to the implant, the more it deforms. This connection utilized the importance of physiological loads during the design of the implant. Therefore, ensuring the implant can distribute loads effectively can improve the stability and longevity of the implant. Figure 7 demonstrates the graphical representation of the hip implant's total deformation percentage in four different loading conditions. The horizontal axis represents the various loading conditions, and the vertical axis represents the total deformation percentage of the hip implant as the loads change. It was found that during jogging, the hip implant achieves the maximum deformation compared to the other three.

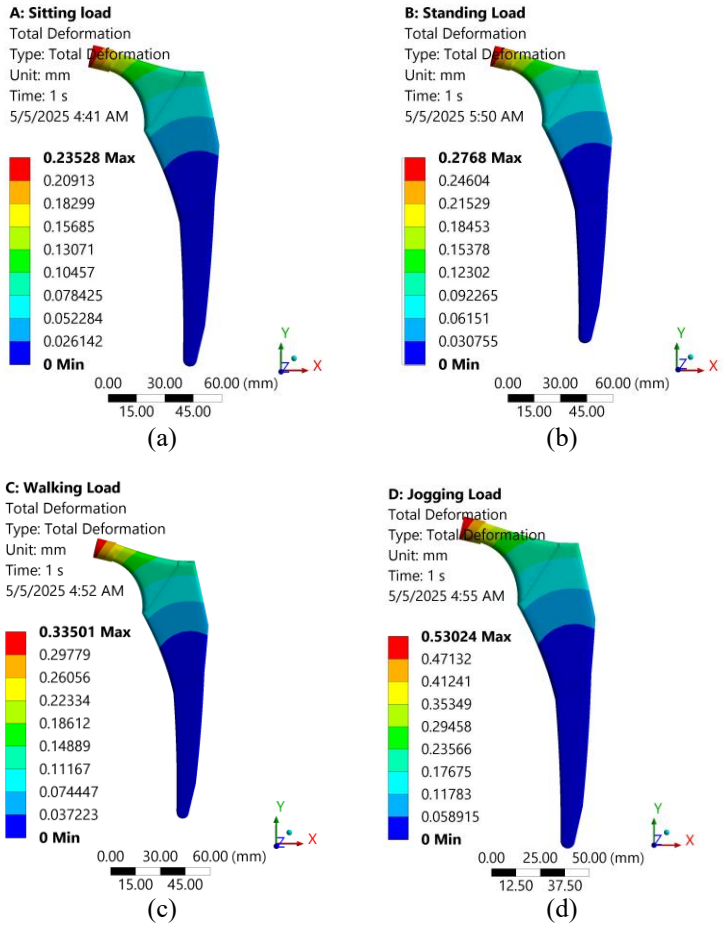

Figure 6. Total deformation of the hip implant in four different loads: (a) Sitting, (b) Standing, (c) Walking, and (d) Jogging

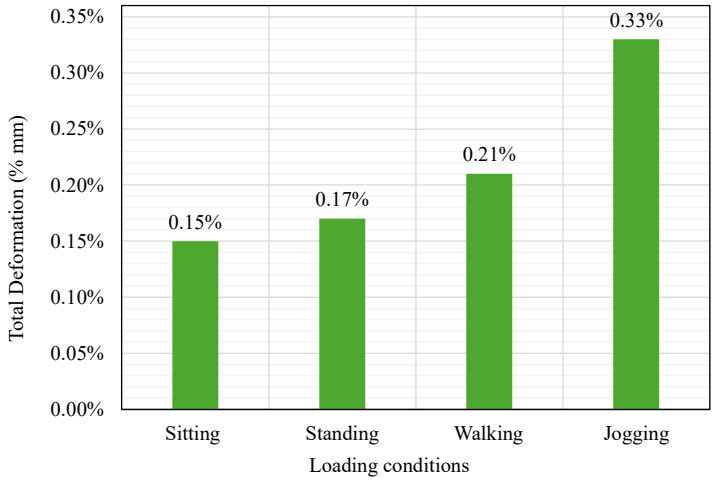

Figure 7. Total deformation in four different loading conditions

The results indicate that the total deformation of the hip implant is higher during jogging due to the higher force acting on the body compared to other conditions, such as sitting, walking, and standing. Therefore, the higher deformation of this study suggests the need for a design without uncertainty. Increasing deformation can sometimes cause hip implant failure, patient discomfort, and reduced mobility. In this regard, understanding the deformation of these physiological activities is essential to ensure the implant design can adapt to a limit of motion, including high-impact loads such as jogging, without compromising structural integrity. This knowledge enables engineers and medical professionals to select materials and optimize implant designs for various patient demographics. It will also help to design the hip implant based on the patient's specific needs, thereby reducing implant failure over time. However, in this study, the hip implant experiences a maximum deformation of 0.33% during jogging, which is considered safe because this small amount of deformation results in less von Mises stress and shear stress than the material's yield strength and shear strength. The implant's von Mises stress and shear stress are discussed in the following subsection. In summary, total deformation analysis is a fundamental part of the design and evaluation of hip implants. This ensures that the implant can maintain its structural integrity and functionality, from lower-impact activities like sitting to high-impact activities like jogging.

3.2 Equivalent Stress

Figure 8 represents the equivalent stress (von Mises) of hip implants under four different loading conditions: sitting load, standing load, walking load, and jogging load. The results for maximum equivalent stress for sitting are 288.83 MPa, for standing is 339.8 MPa, for walking is 423.73 MPa, and for jogging is 650.93 MPa. It is observed that the maximum equivalent stress of hip implants increases with the increase in applied physiological loads. The continuously increasing stress on the loads underscores the importance of understanding the strength and function of implants. It also indicates the need for strong materials and creative design so that the implant can handle those kinds of physiological loads without breaking. Understanding the effect of stress on hip implants under different loading conditions helps design more cost-effective and biocompatible implants. Additionally, Figure 9 below presents the graphical representation of the maximum equivalent stress of a hip implant under four different loading conditions. The horizontal axis represents the various loading conditions, and the vertical axis represents the corresponding maximum equivalent stress of the hip implant. It is found that during jogging, the hip implant achieves the maximum equivalent stress compared to the other three.

The results indicate that the hip implant experiences maximum equivalent stress during jogging as compared to sitting and walking. This is because the hip implant experiences maximum repetitive force during jogging compared to other activities. Compared to walking, it experiences moderate equivalent stress due to the lower impact force. The maximum equivalent von Mises stress indicates the need for a design that can withstand cyclic loads without failure or deformation. The equivalent von Mises stress is a crucial parameter for evaluating the structural performance of the hip implant under various physiological loading conditions. It helps engineers predict the material yield so that it won't fail under certain conditions. The high equivalent stress during jogging can be attributed to repetitive impact forces, which exert significant stress on the implant material. From this perspective, the use of AM materials, such as Ti-6Al-4V, is significant due to their excellent fatigue resistance. In this study, the maximum equivalent von Mises stress is 650.93 MPa lower than the material yield strength. This indicates the hip implant will be considered safe under these applied physiological loads. In summary, the equivalent stress analysis is an essential component of implant evaluation. This ensures that the material and design can endure physiological loads during daily routine and high-impact activities.

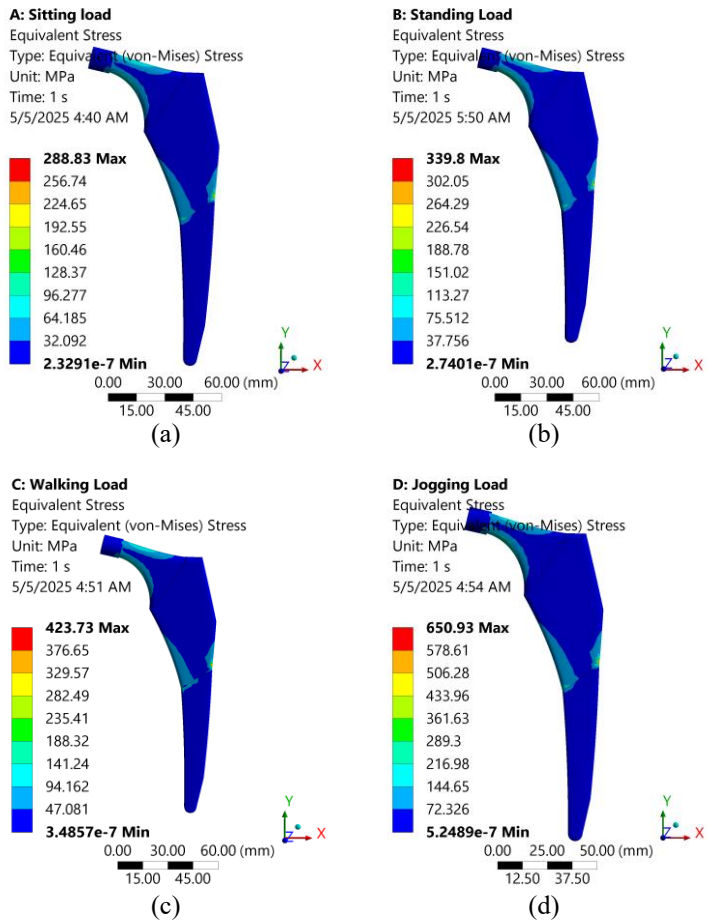

Figure 8. Maximum equivalent stress of hip implant in four different loads: (a) Sitting, (b) Standing, (c) Walking, and (d) Jogging

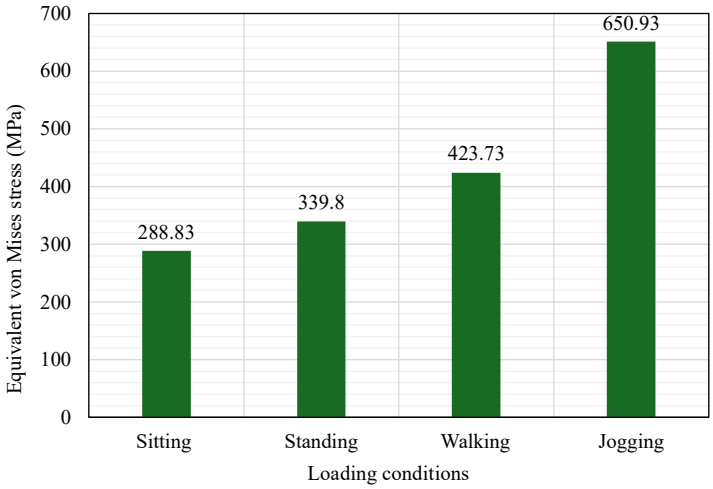

Figure 9. Maximum equivalent stress in four different loading conditions

3.3 Shear Stress

Figure 10 represents the shear stress of hip implants under four different loading conditions, which are the sitting load, standing load, walking load, and jogging load. Where sitting time maximum shear stress is 59.738 MPa, standing time maximum shear stress is 70.28 MPa, walking time maximum shear stress is 84.556 MPa, and jogging time maximum shear stress is 134.63 MPa. It is observed that the maximum shear stress of hip implants increases with the increase in applied physiological loads. This highlights the importance of designing hip implants with consideration for stress distribution. Therefore, the implant can easily withstand the increasing stress levels to prevent failure and deformation of the hip implants, thereby increasing longevity. Additionally, Figure 11 presents a graphical representation of the maximum shear stress of a hip implant under four different loading conditions. The horizontal axis represents the various loading conditions, while the vertical axis represents the corresponding maximum shear stress of the hip implant. It is found that during jogging, the hip implant achieves the maximum shear stress compared to the other three implants.

The results indicate that the hip implant experiences maximum shear stress during jogging, while walking produces moderate shear stress, and walking produces the minimum shear stress. Jogging produces maximum shear stress because of its continuous lateral rotational and axial forces acting on the hip implant. These forces can cause stress levels, especially in critical areas such as the neck of the implant or the connection between the implant and bone. It is essential to manage stress concentrations, as they can cause damage, such as microcracks that can spread over time and compromise the implant's structural integrity. By evaluating shear stress, engineers can identify potential weaknesses in the implant design and make necessary adjustments to enhance its performance under various loading conditions. In summary, assessing shear stress is an important component of designing and evaluating hip implants. This ensures that the implant can withstand lateral and rotational forces while maintaining its structural integrity, thereby enhancing the patient's mobility. The findings of this study highlight the importance of understanding the material's shear stress while designing the hip implant using AM. In this study, the maximum shear stress experienced during jogging is 134.630 MPa, which is lower than the material's shear strength. This means the implant will not experience any shear failure during the maximum load applied.

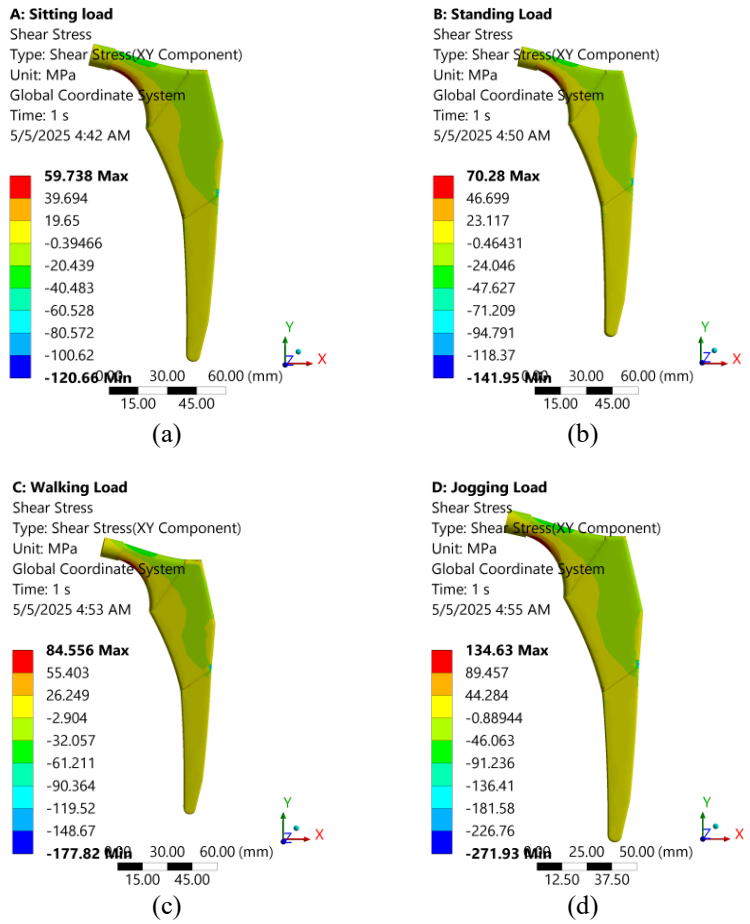

Figure 10. Maximum shear stress of hip implant in four different loads: (a) Sitting, (b) Standing, (c) Walking, and (d) Jogging

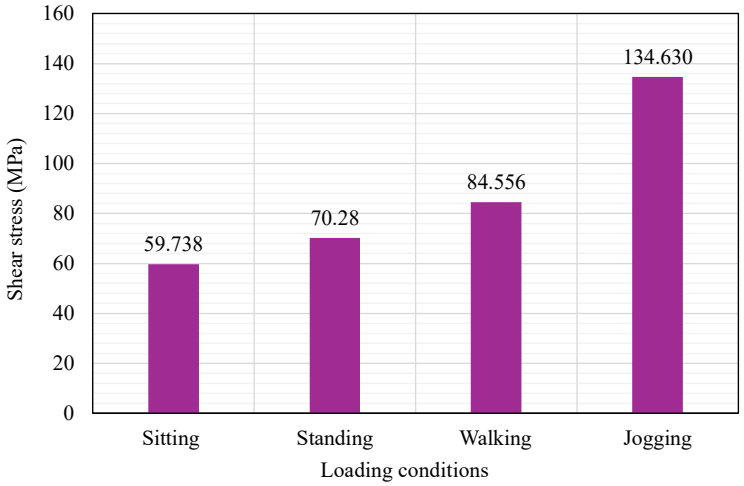

Figure 11. Maximum shear stress in four different loading conditions

4. CONCLUSIONS

This research has shown the significant potential of utilizing AM materials for hip implants using FEA. Through the use of FEA, the stress distribution and deformation behavior in these implants, when subjected to various loading conditions, are simulated and analyzed. This study helps to understand the behavior of hip implants under physiological loads and the design of hip implants within safe parameters. The results of the study show that the total deformation percentage at four different loadings is as follows: sitting, 0.15%; standing, 0.17 mm; walking, 0.21%; and jogging, 0.33%. Similarly, the equivalent von Mises stresses of the hip implant were 288.83 MPa while sitting, 339.8 MPa while standing, 423.73 MPa while walking, and 650.93 MPa while jogging. Additionally, the shear stresses for the hip implant were measured as follows: sitting, 59.738 MPa; standing, 70.28 MPa; walking, 84.556 MPa; and jogging, 134.630 MPa. These results indicate that the total deformation, equivalent stress, and shear stress of hip implants are directly proportional to the applied physiological load acting on the implant head. In this study, the highest equivalent von Mises stress and shear stress were recorded during the jogging time, which is less than the material's yield strength. Similarly, the shear stress is less than the material's shear strength, indicating that the design is safe under physiological loadings. The result was validated with the previous studies to confirm the continuity of this study. However, the findings demonstrated that hip implants constructed from AM materials provide advantageous biomechanical compatibility, hence decreasing the likelihood of implant malfunction and enhancing patient outcomes. Furthermore, the use of AM techniques enables the customization of implants, resulting in improved conformability and more efficient load distribution. The stress studies in the analysis help design the hip implant to reduce mechanical stress, thereby mimicking the mechanical behavior of the femoral bone. The higher stresses can cause implant loosening and failure over time due to the stress-shielding effect. The stress shield occurs when the implant becomes stiffer compared to the surrounding bone, allowing it to withstand a large amount of physiological loads. In this regard, it is essential to study the implant stress behavior to design a hip implant that can minimize stress shielding. Future research can focus on designing hip implants with an understanding of their structural behavior, while reducing stress-shielding effects. In summary, the use of AM materials in the production of hip implants, combined with the application of reliable FEA, is a significant development in the field of orthopedic surgery. This provides a pathway to hip replacement options that are more specific and efficient, strengthening the importance of ongoing studies and advances in this domain.

ACKNOWLEDGEMENTS

The author would like to acknowledge the Malaysian Ministry of Higher Education under the Fundamental Research Grant Scheme FRGS/1/2023/TK10/UMP/02/7 (university reference RDU230104) and Universiti Malaysia Pahang Al-Sultan Abdullah (RDU220367 and PGRS220386) for financial support. The authors would like to thank UMPSA for allowing the research to be conducted using high-performance computers.

CONFLICT OF INTEREST

The authors declare that they have no conflicts of interest.

AUTHORS CONTRIBUTION

A.A. Noman (Conceptualization; Methodology; Formal analysis; Software; Writing – original draft)

M.S. Shaari (Conceptualization; Methodology; Acquisition of funds; Resources; Supervision; Writing - review & editing)

M.R.M Akramin (Writing - review & editing)

K.S. Tan (Writing - review & editing)

AVAILABILITY OF DATA AND MATERIALS

The analysis data, findings, and other supporting documents will be available on request from the corresponding author.

ETHICS STATEMENT

This study was conducted in accordance with the ethical guidelines of Universiti Malaysia Pahang and Al-Sultan Abdullah. This study did not involve any human instruction or hazardous substances, so formal ethical approval was not required.

REFERENCES

[1] T. Kermavnar, A. Shannon, K. J. O'Sullivan, C. McCarthy, C. P. Dunne, L. W. O'Sullivan, "Three-dimensional printing of medical devices used directly to treat patients: A systematic review," *3D Printing and Additive Manufacturing*, vol. 8, pp. 366–408, 2021.

[2] M. E. Shehata, K. B. Mustapha, E. M. Shehata, "Finite element and multivariate random forests modelling for stress shield attenuation in customized hip implants," *Forces in Mechanics*, vol. 10, p. 100151, 2023.

[3] A. A. Noman, M. S. Shaari, H. Mehboob, A. H. Azman, "Recent advancements in additively manufactured hip implant design using topology optimization technique," *Results in Engineering*, vol. 25, p. 103932, 2025.

[4] T. D. Ngo, A. Kashani, G. Imbalzano, K. T. Q. Nguyen, D. Hui, "Additive manufacturing (3D printing): A review of materials, methods, applications and challenges," *Composites Part B: Engineering*, vol. 143, pp. 172–196, 2018.

[5] S. M. Fijul Kabir, K. Mathur, A. Fattah M. Seyam, "A critical review on 3D printed continuous fiber-reinforced composites: History, mechanism, materials and properties," *Composite Structures*, vol. 232, pp. 1–24, 2020.

[6] S. P. Tan, M. A. Ramlan, M. S. Shaari, A. Takahashi, M. R. M. Akramin, "Microstructural and mechanical characterization of AlSi10Mg additively manufactured material using direct metal laser sintering technique," in *Technological Advancement in Mechanical and Automotive Engineering*, pp. 349–360, 2023.

[7] M. Touri, F. Kabirian, M. Saadati, S. Ramakrishna, M. Mozafari, "Additive manufacturing of biomaterials − The evolution of rapid prototyping," *Advanced Engineering Materials*, vol. 21, p.1800511, 2019.

[8] N. Vidakis, C. David, M. Petousis, D. Sagris, N. Mountakis, A. Moutsopoulou, "The effect of six key process control parameters on the surface roughness, dimensional accuracy, and porosity in material extrusion 3D printing of polylactic acid: prediction models and optimization supported by robust design analysis," *Advances in Industrial and Manufacturing Engineering*, vol. 5, p.100104, 2022.

[9] D. Savio, A. Bagno, "When the total hip replacement fails: A review on the stress-shielding effect," *Processes*, vol. 10, pp. 1–17, 2022.

[10] A. Bandyopadhyay, I. Mitra, S. B. Goodman, M. Kumar, S. Bose, "Improving biocompatibility for next generation of metallic implants," *Progress in Materials Science*, vol. 133, p. 101053, 2023.

[11] L. Guo, S. Ataollah Naghavi, Z. Wang, S. Nath Varma, Z. Han, Z. Yao, et al., "On the design evolution of hip implants: A review," *Materials & Design*, vol. 216, p. 110552, 2022.

[12] M. Feyzi, K. Fallahnezhad, M. Taylor, R. Hashemi, "A review on the finite element simulation of fretting wear and corrosion in the taper junction of hip replacement implants," *Computers in Biology and Medicine*, vol. 130, p. 104196, 2021.

[13] H. McKellop, I. Clarke, K. Markolf, H. Amstutz, "Friction and wear properties of polymer, metal, and ceramic prosthetic joint materials evaluated on a multichannel screening device," *Journal of Biomedical Materials Research*, vol. 15, no. 5, pp. 619–653, 1981.

[14] M. Merola, S. Affatato, "Materials for hip prostheses: A review of wear and loading considerations," *Materials*, vol. 12, p.495, 2019.

[15] F. Y. Chin, M. S. Shaari, A. Takahashi, M. R. M. Akramin, S. Urai, "Fatigue crack growth behavior of AlSi10Mg material produced by direct metal laser sintering using s-version finite element method," *Journal of Failure Analysis and Prevention*, vol. 23, no. 2, pp. 601–608, 2023.

[16] P. Jhunjhunwala, A. Kishor, R. G. Burela, R. Singh, A. Gupta, "Finite element analysis and topology optimization of Ti-6Al-4V hip implant fabricated by laser powder bed fusion process," *Proceedings of the Institution of Mechanical Engineers, Part E: Journal of Process Mechanical Engineering*, p. 09544089221144189, 2022.

[17] T. Lee, S. Lee, I. S. Kim, Y. H. Moon, H. S. Kim, C. H. Park, "Breaking the limit of Young's modulus in low-cost Ti–Nb–Zr alloy for biomedical implant applications," *Journal of Alloys and Compounds*, vol. 828, p. 154401, 2020.

[18] M. A. Azri, M. S. Shaari, A. Kamal Ariffin, S. Abdullah, "Microstructure, mechanical properties and fatigue behavior of AlSi10Mg: an additive manufacturing material," *International Journal of Engineering & Technology*, vol. 7, pp. 186–190, 2018.

[19] M. Ceddia, B. Trentadue, G. De Giosa, G. Solarino, "Topology optimization of a femoral stem in titanium and carbon to reduce stress shielding with the FEM method," *Journal of Composites Science*, vol. 7, no. 7, 2023.

[20] Z. Yang. Finite Element Analysis for Biomedical Engineering Applications. 1st ed. Boca Raton: CRC Press, 2019.

[21] K. N. Chethan, N. Shyamasunder Bhat, M. Zuber, B. Satish Shenoy, "Static structural analysis of different stem designs used in total hip arthroplasty using finite element method," *Journal of Biomedical Physics and Engineering*, vol. 9, no. 5, pp. 507–516, 2019.

[22] P. K. Mishra, B. Karthik, T. Jagadesh, "Finite element modelling and experimental investigation of tensile, flexural, and impact behaviour of 3D-printed polyamide," *Journal of The Institution of Engineers (India): Series D*, vol. 105, no. 1, pp. 275–283, 2024.

[23] R. Rahchamani, R. Soheilifard, "Three-dimensional structural optimization of a cementless hip stem using a bi-directional evolutionary method," *Computer Methods in Biomechanics and Biomedical Engineering*, vol. 23, no. 1, pp. 1–11, 2020.

[24] F. Eltit, Q. Wang, R. Wang, "Mechanisms of adverse local tissue reactions to hip implants," *Frontiers in Bioengineering and Biotechnology*, vol. 7, no. 176, pp. 1–17, 2019.

[25] C. K N, G. Ogulcan, S. Bhat N, M. Zuber, S. Shenoy B, "Wear estimation of trapezoidal and circular shaped hip implants along with varying taper trunnion radiuses using finite element method," *Computer Methods and Programs in Biomedicine*, vol. 196, p. 105597, 2020.

[26] C. X. Wei, M. F. Burrow, M. G. Botelho, H. Lam, W. K. Leung, "In vitro salivary protein adsorption profile on titanium and ceramic surfaces and the corresponding putative immunological implications," *International Journal of Molecular Sciences*, vol. 21, no. 9, pp. 1–17, 2020.

[27] A. H. Chern, P. Nandwana, T. Yuan, M. M. Kirka, R. R. Dehoff, P. K. Liaw, et al., "A review on the fatigue behavior of Ti-6Al-4V fabricated by electron beam melting additive manufacturing," *International Journal of Fatigue*, vol. 119, no. May, pp. 173–184, 2019.

[28] A. E. Ismail, A. K. Ariffin, S. Abdullah, M. J. Ghazali, "Finite element analysis of j-integral for surface cracks in round bars under combined mode I loading," *International Journal of Integrated Engineering*, vol. 9, no. 2, 2017.

[29] M. R. M. Akramin, A. K. Ariffin, M. Kikuchi, M. Beer, M. S. Shaari, M. N. M. Husnain, "Surface crack growth prediction under fatigue load using probabilistic S-version finite element model," *Journal of the Brazilian Society of Mechanical Sciences and Engineering*, vol. 40, no. 11, p. 522, 2018.

[30] O. M. Al-Moayed, A. K. Kareem, A. E. Ismail, S. Jamian, M. N. Nemah, "Distribution of mode I stress intensity factors for single circumferential semi-elliptical crack in thick cylinder," *International Journal of Integrated Engineering*, vol. 11, no. 7, pp. 102–111, 2019.

[31] M. S. Shaari, A. K. Ariffin, A. Takahashi, S. Abdullah, M. Kikuchi, M. R. M. Akramin, "Fatigue crack growth analysis on square prismatic with embedded cracks under tension loading," *Journal of Mechanical Engineering and Sciences*, vol. 14, no. 1, pp. 2511–2525, 2017.

[32] K. N. Chethan, M. Zuber, B. N. Shyamasunder, S. B. Satish, "Optimized trapezoidal-shaped hip implant for total hip arthroplasty using finite element analysis," *Cogent Engineering*, vol. 7, no. 1, p. 1719575, 2020.

[33] N. Premkumar, K. Subhashini, G. Valarmathi, J. Kumar, S. Meganathan, ''Numerical analysis of hip bone replacement design parameters'', *Materials Today: Proceedings*, vol. 46, pp. 4271–4277, 2020.

[34] E. Tyflopoulos, M. Steinert, "A comparative study of the application of different commercial software for topology optimization," *Applied Sciences (Switzerland)*, vol. 12, no. 2, p. 611, 2022.

[35] S. A. Naghavi, M. Tamaddon, P. Garcia-Souto, M. Moazen, S. Taylor, J. Hua, et al., "A novel hybrid design and modelling of a customised graded Ti-6Al-4V porous hip implant to reduce stress-shielding: An experimental and numerical analysis", *Frontiers in Bioengineering and Biotechnology*, vol. 11, no. 1, pp. 1–20, 2023.

[36] G. Bergmann, A. Bender, J. Dymke, G. Duda, P. Damm, "Standardized loads acting in hip implants," *PLOS ONE*, vol. 11, no. 5, p. e0155612, 2016.